A simple method of solving the spectral problem $L^*\zeta_0 = 0$, $\zeta_0 = 0$ ($z = 0, -H$) is presented in [3]. The Brunt–Väisälä frequency in this method is approximated by a piecewise-constant function, i.e., the whole interval of values $[-H, 0]$ is divided into layers, in each of which the solution is written down in analytic form and the integration of (8) is reduced to converting the function and its derivative or the impedance $Z = \zeta_0/\zeta_{0z}'$ from one horizon to another over the whole layer. Then the equation for the eigenvalues has the form $Z_{0J} - Z_{-H}^J = 0$, where Z_{-H}^J is the impedance converted from the bottom to the J-th horizon, while Z_0^J is the impedance converted from the surface to the same horizon. The number of the eigennumber is determined by the number of zeros at the appropriate eigenfunction. Integration of (9) is performed by an analogous method, the solution in each layer is expressed in terms of the solution of the homogeneous equation and the right side of (9). A program is written on the basis of this method and the "exact" and approximate methods are compared. It is shown that for real (practically for all stable) flows the relative error in determining the coordinates of the leading fronts by using the perturbation method for the first modes does not exceed 10% (this is totally adequate for the processing of full-scale data).

As an illustration of the influence of shear flows on internal waves, the leading wave fronts of the first and second internal wave modes are represented in Fig. 2 for a medium with a two-dimensional shear flow (solid curve). The distributions of the Brunt–Väisälä frequency and the flow velocity components were taken from results of measurements and are presented in Figs. 3 and 4. Corresponding fronts for media without flows are shown by dashed lines for comparison.

It is seen from Figs. 1 and 2 that the presence of flows results in a substantial change in the wave front location, and therefore, of the whole internal wave field also. These changes can be computed by using the presented sufficiently accurate and simple algorithm.

LITERATURE CITED

1. Yu. Z. Miropol'skii, Dynamics of Internal Gravitational Waves in the Ocean [in Russian], Gidrometeoizdat, Leningrad (1981).
2. V. A. Borovikov and E. S. Levchenko, "Green's function of the internal wave equation in a stratified fluid layer with mean shear flows," in: Waves and Diffraction [in Russian], Vol. 1, Tbilisi (1985).
3. V. V. Goncharov, "On certain features of internal waves in the ocean," in: Tsunami and Internal Waves [in Russian], Sevastopol' (1976).

DISPLACING OIL WITH HOT WATER AND STEAM

A. F. Zazovskii

UDC 532.546+622.276.65

Exact solutions are derived via the approach of [1-3] for frontal oil displacement by steam or steam–water mixtures [4] in the large-scale approximation, i.e., where we neglect capillary, diffusion, and nonequilibrium effects as well as thermal conduction in the stratum in the displacement direction. It is assumed that the water and steam when present together in the porous medium have equal mobilities. Then three-phase flows, if they occur, amount to two-phase ones, with the aqueous phase a mixture of water and steam. The thermal-wave structure is determined by the nonlinear temperature dependence for the specific heat content in the generalized water phase, which is independent of the saturation distribution. For example, if saturated steam is pumped into the stratum, the temperature alters stepwise, with the step corresponding to the steam condensing to cold water. In superheated-steam displacement, there is a two-stage temperature distribution, with a slow front in which the steam cools to the transition point and a more rapid condensation one. The relation between the displacing capacity and the specific heat content is of turning-point type: it is maximal for hot water and decreases on going to cold water and steam. Therefore, one cannot construct the solution in the large-scale approximation without considering the internal step structure corresponding to the condensation front, where the evolutionary conditions are not obeyed. The condition for a continuous internal structure is related to the diffuseness in

Moscow. Translated from Zhurnal Prikladnoi Mekhaniki i Tekhnicheskoi Fiziki, No. 6, pp. 97-107, November-December, 1987. Original article submitted July 28, 1986.

the thermal front arising from conduction, and this gives additional conditions that eliminate the arbitrary element in constructing the saturation distribution. This simulation method, although clearly approximate, reproduces the characteristic features of steam treatment.

1. Formulation. The following system describes the one-dimensional displacement of oil by steam when one neglects hydrocarbon extraction into the gas phase:

$$v_i = -k(f_i/\mu_i)\partial p/\partial x \quad (i = 1, 2, 3); \tag{1.1}$$

$$m\frac{\partial}{\partial t}(s_1\rho_1 + s_3\rho_3) + \frac{\partial}{\partial x}(\rho_1 v_1 + \rho_3 v_3) = 0,$$

$$m\frac{\partial}{\partial t}(s_2\rho_2) + \frac{\partial}{\partial x}(\rho_2 v_2) = 0, \quad m\frac{\partial}{\partial t}\sum_{i=1}^{3} s_i\rho_i U_i + \frac{\partial}{\partial t}(c_4 T) + Q = 0; \tag{1.2}$$

$$Q = \frac{\partial}{\partial x}(q_c + q_T) + P,$$

$$q_c = \sum_{i=1}^{3}\rho_i h_i v_i, \quad q_T = -\lambda\frac{\partial T}{\partial x}, \quad P = a(T - T_0); \tag{1.3}$$

$$\sum_{i=1}^{3} s_i = 1, \quad \rho_1 = \text{const}, \quad \rho_2 = \text{const}, \quad \rho_3 = p/RT,$$

$$U_i = h_i - p/\rho_i, \ \rho_1 h_1 = c_1 T, \ \rho_2 h_2 = c_2 T, \ \rho_1 h_3 = c_1 T + \varkappa, \tag{1.4}$$

$$f_i = f_i(s_1, s_3, T) \ (i = 1, 2, 3), \ \mu_j = \mu_j(T) \ (j = 1, 2), \ \mu_3 = \mu_3(T, p).$$

Here x is a coordinate, t time, m porosity, k permeability, p pressure, T temperature, s_i saturation, f_i relative permeability, μ_i viscosity, ρ_i density, v_i infiltration rate, h_i and U_i the specific heat content and internal energy of phase i, with subscript i = 1 referring to water, i = 2 to oil, and i = 3 to steam, Q heat-transfer rate, R specific gas constant for steam, $\varkappa$ latent heat of evaporation, λ stratum thermal conductivity, c_1, c_2, and c_4 bulk specific heats of water, oil, and rock, a heat-transfer coefficient per unit stratum volume, and T_0 surrounding rock temperature.

Equations (1.1) express D'Arcy's law, with (1.2) representing the balances for water and steam, oil, and the amount of heat in the flow. The heat-influx equation (1.3) incorporates the heat fluxes due to convection q_C and conduction q_T, as well as the heat-transfer rate between the stratum and the surrounding rocks P in accordance with Newton's law. Equations (1.4) indicate that thermal expansion in the liquids is neglected, while the steam is considered as an ideal gas. Here λ, $\varkappa$, and T_0 are taken as constant.

For simplicity, we neglect the difference between the internal energy U_i and the enthalpy h_i for each phase on the basis that $U_i = h_i$ (i = 1, 2, 3). This is justified for the liquid phases (i = 1, 2) because $\Delta_i = (h_i - U_i)/h_i \ll 1$. For steam, $\Delta_3 \approx 0.2$-0.3, but as the density of steam is low, the corresponding contribution to the heat content for a volume element in the porous medium is very small.

System (1.1)-(1.4) is closed either by the conditions for water and steam equilibrium or by the equations for the evaporation and condensation kinetics. In the first case, we have as follows, where $T_*(p)$ is the phase-transition temperature:

$$s_3 = 0 \quad (T < T_*), \quad s_1 = 0 \quad (T > T_*), \quad 0 \leqslant s_1 + s_3 \leqslant 1 \quad (T = T_*). \tag{1.5}$$

In the second case, the mass phase-transition rate Ω is usually taken as proportional to the difference between the saturation pressure $p_*(T)$ and the pressure p [5]. We take Ω as the rate of change in the water mass in unit volume of the porous medium to get

$$\frac{\partial}{\partial t}(m\rho_1 s_1) = \Omega(T, s_1, s_3) = \omega(s_1, s_3, T)[p_*(T) - p],$$
$$\omega > 0 \quad (s_3 > 0, \quad T \leqslant T_* \quad \text{or} \quad s_1 > 0, \quad T \geqslant T_*), \tag{1.6}$$
$$\omega = 0 \quad (s_1 = 0, \quad T > T_* \quad \text{or} \quad s_3 = 0, \quad T < T_*).$$

Here $\omega(s_1, s_3, T)$ is a known function, while the conditions as equalities and inequalities incorporate the fact that the phase transition rate becomes zero for superheated steam ($s_1 = 0$, $T > T_*$) and underheated liquid ($s_3 = 0$, $T < T_*$).

We neglect the effects from pressure change in the stratum on the phase state of the water and the viscosity of the steam, taking $p = p_*(T_*) = \text{const}$ in (1.5) and (1.6). We eliminate p from (1.2) to get

$$v_i = UF_i, \quad F_i = \frac{f_i}{\mu_i}\left(\sum_{j=1}^{3}\frac{f_j}{\mu_j}\right)^{-1} \quad (i = 1, 2, 3). \tag{1.7}$$

Frontal displacement corresponds to the solution to the above system with the initial and boundary conditions

$$\begin{gathered} s_1 = s_0, \quad s_3 = 0, \quad T = T_0 < T_* \quad (t = 0, \quad x > 0), \\ s_1 = s_1^0, \quad s_3 = s_3^0, \quad T = T^0 \geqslant T_*, \quad U = U^0 \quad (t > 0, \quad x = 0), \end{gathered} \tag{1.8}$$

where s_0 is the initial water level in the stratum, T^0 and U^0 are the temperature and infiltration rate for the pumped mixture, and s_1^0 and s_3^0 are the volume concentrations of water and steam in it. When superheated steam is used, $s_1^0 = 0, s_3^0 = 1, T^0 > T_*$, while for saturated steam, $s_1^0 = 0, s_3^0 = 1, T^0 = T_*$, and for a mixture of hot water and steam, $s_1^0 + s_3^0 = 1, T^0 = T_*$, while for hot water alone, $s_1^0 = 1, s_3^0 = 0, T^0 \leqslant T_*$.

2. Two-Phase Large-Scale Approximation. We introduce the volume steam concentration in the fictitious water phase c, while the viscosity and relative permeability for the aqueous phase are defined by $\mu_1^* = (1 - c)\mu_1 + c\mu_3$ and $f_1^* = (1 - c)f_1 + cf_3$, with the saturation and the fraction in the flow denoted correspondingly by s and $F = F(s, T, c)$. Then

$$\begin{gathered} s_1 = (1 - c)s, \; s_2 = 1 - s, \; s_3 = cs, \; F_1 = (1 - c)F, \; F_2 = 1 - F, \\ F_3 = cF \end{gathered} \tag{2.1}$$

and (1.2) and (1.6) after conversion to dimensionless variables and use of (1.4), (1.7), and (2.1) become

$$\begin{gathered} \frac{\partial}{\partial\tau}(Ks) + \frac{\partial}{\partial X}(\Lambda KF) = 0, \quad \frac{\partial}{\partial\tau}(1 - s) + \frac{\partial}{\partial X}[\Lambda(1 - F)] = 0, \\ \frac{\partial}{\partial\tau}[T'(As + b)] + \frac{\partial}{\partial X}[\Lambda T'(AF + h)] + a'T' = \varepsilon\frac{\partial^2 T}{\partial X^2}; \end{gathered} \tag{2.2}$$

$$\begin{gathered} \frac{\partial}{\partial\tau}[s(1 - c)] = \frac{1}{\nu}\Omega(T, c, s) = \omega'\left[p_*'(T') - 1\right], \\ p_*'(T_*') = 1, \quad \omega' > 0 \; (c > 0, \; T' \leqslant T_*' \text{ or } c < 1, \; T' \geqslant T_*'), \\ \omega' = 0 \; (c = 1, \; T' > T_*' \text{ or } c = 0, \; T' < T_*'); \end{gathered} \tag{2.3}$$

$$\begin{gathered} X = \frac{x}{L}, \quad \tau = \frac{U^0 t}{mL}, \quad \Lambda = \frac{U}{U^0}, \quad T' = \frac{T - T_0}{\Delta T}, \quad T_*' = \frac{T_* - T_0}{\Delta T}, \quad p_*' = \frac{p_*}{p}, \\ \varepsilon = \frac{\lambda}{LU^0(c_1 - c_2)}, \quad \nu = \frac{U^0\rho_1}{Lp\omega_*}, \quad a' = \frac{aL}{U^0(c_1 - c_2)}, \quad b = \frac{c_2 + c_4/m}{c_1 - c_2}, \\ h = \frac{c_2}{c_1 - c_2}, \quad \varkappa' = \frac{\varkappa}{c_1\Delta T}, \quad \omega' = \frac{\omega}{\omega_*}, \quad D(T') = \frac{c_1}{c_1 - c_2}\left[1 - \left(1 + \frac{\varkappa'}{T'}\right)B\right], \\ B(T') = \frac{B_0}{T' + \Theta}, \quad B_0 = \frac{p}{R\rho_1\Delta T}, \quad \Theta = \frac{T_0}{\Delta T}, \quad \omega_* = \omega(1/2, 1/2, T_*), \\ K(c, T) = 1 - (1 - B)c, \; A(c, T) = 1 - Dc, \; \Delta T = T^0 - T_0, \end{gathered} \tag{2.4}$$

with K^{-1} the thermal-expansion coefficient for the aqueous phase, which incorporates the evaporation, condensation, and steam expansion, and L is the characteristic stratum dimension.

In what follows, the primes to the dimensionless variables are omitted and no misunderstanding can arise. Then (1.8) becomes

$$\begin{gathered} s = s_0, \; c = 0, \; T = 0 \; (\tau = 0, \; X > 0), \\ s = 1, \; c = c^0, \; T = 1, \; \Lambda = 1 \; (\tau > 0, \; X = 0). \end{gathered} \tag{2.5}$$

Equations (2.2) and (2.3) contain two small parameters: ε and ν, where ε^{-1} is the Peclet number, which characterizes the ratio of the convective heat flux to the conductive one, while ν is the ratio of the characteristic evaporation (condensation) time to the characteristic displacement time mL/U^0. We take $\varepsilon = \nu = 0$ to get a formulation corresponding to the large-scale approximation. Here $\Omega \equiv 0$, and (2.3) becomes the phase-equilibrium conditions

$$c = 0 \; (T < T_*), \quad c = 1 \; (T > T_*), \quad 0 \leqslant c \leqslant 1 \; (T = T_*), \tag{2.6}$$

and the flow-distribution function becomes a function of two variables: s and the dimensionless specific heat content of the water phase H(T, c):

$$F = F(s, H), \quad H(T, c) = \frac{T(A+h)}{K} = \frac{c_1[T(1-c)+(T+\varkappa)B(T)c]}{(c_1-c_2)[1-c+B(T)c]}. \tag{2.7}$$

Experiment [6] indicates that the H dependence of F is not monotone for heavy viscous oils†: the proportion of the aqueous phase in the flow decreases when the water is heated to the transition temperature mainly on account of increase in the viscosity ratio for the water and oil, and it increases sharply when the water evaporates because of the high steam mobility. Then $F'_H \leqslant 0$ for $T < T_*$ and $F'_H \geqslant 0$ for $T \geqslant T_*$. Figure 1 shows typical F distributions for oil being displaced by steam, hot water, and cold water (lines 1-3). The calculations have been based on (1.7) for the relative phase permeabilities from [6] and displacement conditions close to natural ones: p = 5 MPa, T_0 = 20°C, T_* = 265°C, $\mu_1(T_0)$ = 1 MPa·sec, $\mu_1(T_*)$ = 0.1 MPa·sec, $\mu_3(T_*)$ = 0.01 MPa·sec, $\mu_2(T_0)$ = 200 MPa·sec, and $\mu_2(T_*)$ = 4.4 MPa·sec. The important point however here is not so much the exact forms of curves 1-3 as the disposition of them. The sense of change in H is shown by the arrows along the line OLPN. H(T, c) is important in all the subsequent arguments. The definition of (2.7) and the assumption that the specific heats and the latent heat of evaporation are constant mean that it takes the form of the piecewise-linear line OLPN in the (T, H) plane (Fig. 2). The segments OL and PN are parallel, while the vertical segment LP corresponds to the change in steam concentration c in the aqueous phase from 0 to 1.

With c = 0 and $T < T_*$, (2.4) gives K = A = 1, and system (2.2) and (2.6) coincides with that obtained in [1] for nonisothermal oil displacement by water. With c = 1 and $T > T_*$ we have K = B(T), A = 1 − D(T), and (2.2), (2.6) describe oil displaced by superheated steam. Finally, with $0 \leqslant c \leqslant 1$, $T = T_*$, the K and A are linear functions of c. It is in this range in c and T that the actual three-phase flow is represented as a fictitious two-phase one.

In the large-scale approximation, we have discontinuous distributions for s, c, T, and the dimensionless flow rate Λ, which is due to the equation system being hyperbolic. The discontinuous solution is not uniquely determined by the initial and boundary conditions. We construct it as the limit to a sequence of continuous solutions to the full system as obtained for $\varepsilon, \nu \to 0$. Then the steps will correspond to narrow transition zones, where the variables change rapidly in response to capillary and nonequilibrium effects as well as thermal conduction. The conditions for such zones or internal structure are also called the permissibility or stability conditions, and they distinguish a unique solution corresponding to the correct physical asymptote out of the set of possible ones [7]. The capillary effects are neglected in the initial equations because the structure of the saturation steps is known for T = const and so are the corresponding stability conditions [8].

3. Thermal-Wave Structure. We consider the internal structure in the temperature discontinuity corresponding to the steam condensation front. Let V be the step speed, while $s^{\pm}$, $T^{\pm}$, $c^{\pm}$, $\Lambda^{\pm}$ are the values of the variables after the step (minus) and ahead of it (plus). We transfer to a coordinate system linked to the step, $\eta = (X - V\tau)/\varepsilon$, $\tau' = \tau/\varepsilon$, and let ε and ν tend to zero to get a stationary internal solution that satisfies the linkage conditions to the external solution

$$-V\frac{d}{d\eta}(Ks) + \frac{d}{d\eta}(\Lambda KF) = 0, \quad -V\frac{d}{d\eta}(1-s) + \frac{d}{d\eta}[\Lambda(1-F)] = 0,$$
$$-V\frac{d}{d\eta}[T(As+b)] + \frac{d}{d\eta}[\Lambda T(AF+h)] = \frac{d^2T}{d\eta^2}; \tag{3.1}$$

$$-V\frac{d}{d\eta}[s(1-c)] = \frac{\varepsilon}{\nu}\Omega(T, c, s); \tag{3.2}$$

$$s = s^{\pm}, \; T = T^{\pm}, \; c = c^{\pm}, \; \Lambda = \Lambda^{\pm} \quad (\eta = \pm\infty). \tag{3.3}$$

We integrate (3.1) from $-\infty$ to η and use (3.3) and assume that $dT(-\infty)/d\eta = 0$ to get

$$-V(Ks - K^-s^-) + \Lambda KF - \Lambda^-K^-F^- = 0,$$
$$V(s - s^-) + \Lambda(1-F) - \Lambda^-(1-F^-) = 0,$$
$$-V[T(As+b) - T^-(A^-s^- + b)] + \Lambda T(AF+h) - \Lambda^-T^-(A^-F^- + h) = dT/d\eta, \tag{3.4}$$
$$K^{\pm} = K(c^{\pm}, T^{\pm}), \; A^{\pm} = A(c^{\pm}, T^{\pm}), \; F^{\pm} = F(s^{\pm}, T^{\pm}, c^{\pm}).$$

†This feature was pointed out by K. M. Fedorov, who made the constructions in Fig. 1.

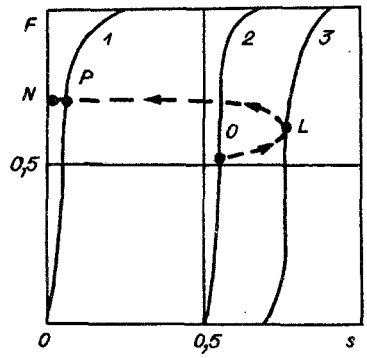

Fig. 1

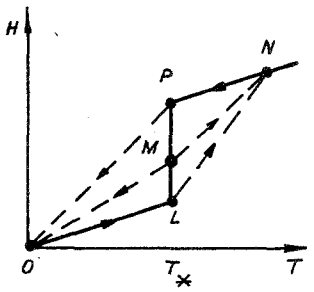

Fig. 2

We transform the first two equations in (3.4) to

$$V = \frac{\Lambda F - \Lambda^- K^- F^-/K}{s - K^- s^-/K}, \quad \Lambda = \Lambda^- - \left(1 - \frac{K^-}{K}\right)(\Lambda^- F^- - V s^-), \tag{3.5}$$

and then eliminate s, F, and Λ from the third, which gives

$$dT/d\eta = (T - T^-)\{\Lambda^- [F^- K^- \Phi + (1 - F^-)h] - V[s^- K^- \Phi + (1 - s^-)h + b - h]\}, \quad \Phi(T, c) = [H(T, c) - H(T^-, c^-)]/(T - T^-). \tag{3.6}$$

From (3.6) and the obvious requirement $(T - T^-)dT/d\eta \geqslant 0$ we have that an internal step structure accompanied by evaporation or condensation requires obedience to the condition

$$\Lambda^- [K^- F^- \Phi + (1 - F^-)h] - V[K^- s^- \Phi + (1 - s^-)h + b - h] \geqslant 0 \tag{3.7}$$

for all T between T^- and T^+; equality occurs in (3.7) only for $T = T^{\pm}$, and otherwise the temperature distribution in the transition zone is not single-valued.

We use the conditions in the step derived by substituting $s = s^+$, $T = T^+$, $c = c^+$, $\Lambda = \Lambda^+$ and $dT(-\infty)/d\eta = 0$ into (3.4) and transform (3.7) to $(F^-/s^- - h/b)(\Phi - \Phi^+) \geqslant 0$, where $\Phi^+ = (H^+ - H^-)/(T^+ - T^-)$. As F has a specific distribution (Fig. 1), $F^-/s^- > h/b$ always in the solutions, so (3.7) finally becomes

$$(H - H^-)/(T - T^-) \geqslant (H^+ - H^-)/(T^+ - T^-). \tag{3.8}$$

One can give an obvious graphical interpretation in the (T, H) plane for (3.8): if the step is to be permissible, the straight-line segment joining the points $(T^{\pm}, H^{\pm})$ on the H(T) curve should not have any other points of intersection with that curve, and it should run above H(T) for $T^- > T^+$ and below it for $T^- < T^+$.

The permissible steps are thus those corresponding to saturated steam condensation, i.e., for $T^- = T_*$, $c^- > 0$, $T^+ < T_*$, and $c^+ = 0$. In the (T, H) plane, they correspond to transitions from points on LP to point O (PO and MO in Fig. 2). The superheated-steam condensation front ($T^- > T_* > T^+$) splits up into two steps: a slow one corresponding to the steam cooling to the transition point and a fast one corresponding to saturated steam condensing to cold water. As segment NP of the H(T) curve is linear (Fig. 2), the slow step is a contact discontinuity, so the characteristic scale of the transition zone increases as $\tau^{1/2}$. The two-front thermal-wave structure is the (T, H) plane corresponds to the kinked line NPO. Similarly, one finds that pumping water into a hot stratum ($T^- \leqslant T_* < T^+$) causes the evaporation front to coincide with the step in temperature from $T^- = T_*$ to T^+ (transitions LN and MN in Fig. 2). Therefore, pumping cold water into the stratum ($T^- < T_*$) results in a slower water-heating front behind the evaporation front, where the temperature rises to the transition point, as illustrated by curve OLN in Fig. 2.

This result appears to have been established first in the single-phase approximation of [9]. Our analysis of the thermal-wave structure is analogous to the study on the concentration step structure in oil displacement by a solution of an active material [2, 10, 11]. Here the thermal conductivity plays the role of component diffusion, while the specific heat content H(T, c) here acts as the reciprocal function for isothermal sorption.

It can however be seen that (3.8) does not completely eliminate the arbitrary element in condensation-front step construction. The nine variables at the step $s^{\pm}$, $T^{\pm}$, $c^{\pm}$, $\Lambda^{\pm}$, and V are defined by three integral-balance equations for water, oil, and the amount of heat in

the flow and two relations between $T^{\pm}$ and $c^{\pm}$, which are consequences of the phase-equilibrium conditions. Three further relations apply to the step on account of the characteristics of (2.2). The latter for $T \neq T_*$ and $T = T_*$ are correspondingly

$$\frac{dX}{d\tau} = \xi_1 = \Lambda F'_s, \quad \frac{ds}{d\tau} + \frac{\Lambda}{\xi_1 - \xi_2}\left[F'_T + \frac{K'}{KW}(1-F)(bF - hs)\right]\frac{dT}{d\eta} = -\frac{a'T}{W}\left[\frac{\Lambda F'_T}{\xi_1 - \xi_2} + \frac{K'_T}{K}(1-F)s\right],$$

$$\frac{dX}{d\tau} = \xi_2 = \Lambda\frac{F + h[K - h(1-K)]^{-1}}{s + b[K - h(1-K)]^{-1}}, \quad \frac{dT}{d\tau} = -\frac{a'T}{W}, \tag{3.9}$$

$$\frac{dX}{d\tau} = \xi_3 = \infty, \quad \frac{d\Lambda}{dX} = -\frac{K'_T}{KW}\left[\Lambda(bF - hs)\frac{dT}{dX} - a'sT\right],$$

$$F'_s = \frac{\partial F}{\partial s}, \quad F'_T = \frac{\partial F}{\partial T}, \quad K'_T = \frac{dK}{dT}, \quad W = [K - h(1-K)]s + b;$$

$$\frac{dX}{d\tau} = \xi_1 = \Lambda F'_s, \quad \frac{ds}{d\tau} + \frac{\Lambda F'_c}{\xi_1 - \xi_2}\frac{dc}{d\tau} = \Psi\left[\frac{\Lambda F'_c}{\xi_1 - \xi_2}\frac{K}{sK'_c} - (1-F)\right], \quad \frac{dX}{d\tau} = \xi_2 = \Lambda\frac{F}{s}, \quad \frac{dc}{d\tau} = -\frac{\Psi K}{sK'_c},$$

$$\frac{dX}{d\tau} = \xi_3 = \infty, \quad \frac{d\Lambda}{dX} = -\Psi = \frac{a'(1-B)}{D - (1+h)(1-B)} = -a'T_*\frac{(c_1 - c_2)(1-B)}{\varkappa B}, \tag{3.10}$$

$$F'_c = \frac{\partial F}{\partial c}, \quad K'_c = \frac{dK}{dc}.$$

Let $\xi_1^{\pm}$ be the characteristic velocities behind the step (minus) and ahead of it (plus), with the step propagating with velocity V; (3.9) and (3.10) imply that the third-family characteristic, which satisfies $dX/d\tau = \xi_3^- > V$ and is therefore called arriving at the step, introduces Λ^-. The inequalities $\xi_2^+ < V < \xi_2^-$ for $\xi_2^{\pm}$ are met by (3.8) (we have $V = \xi_2^{\pm}$ for the temperature steps not involving phase transitions), and the corresponding characteristics introduce T^+ and T^- into the step (or c^-). There are thus eight relations for the nine unknowns. The lacking relation is derived from the condition for an internal step structure.

4. Internal Condensation-Front Structure. From (3.8) we have $T^+ = c^+ = 0$, $T^- = T_*$, $0 < \bar{c} \leq 1$. We seek the condition for a continuous solution $T(\eta)$, $c(\eta)$, $s(\eta)$, and $\Lambda(\eta)$ to the interior problem of (3.1) and (3.2) or in transformed form (3.2), (3.5), and (3.6), which has to satisfy (3.3). Strictly speaking, it is not obvious that there can be a continuous saturation distribution $s(\eta)$ in the absence of a capillary-pressure step, and it needs a demonstration similar to that given in [3] for a similar treatment. In that case, one establishes the existence of a continuous $s(\eta)$ directly as a consequence of continuity in $T(\eta)$ and $c(\eta)$ together with a continuous dependence of s on T and c defined by (3.5). In [3], it is shown that the resulting continuous solution coincides with that obtained on passing to the limit by letting the capillary pressure tend to zero.

As the range in s is limited, we put s = const for simplicity in (3.2). We also assume that the condensation rate $\Omega = O(c^n)$, where $0 < n < 1$ for $c \to 0$ and $T < T_*$. These assumptions have little effect on the essence of the treatment, but they allow us to identify the main features in the interior solution corresponding to the actual physical situation, where nonequilibrium effects are small by comparison with those from thermal conduction.

To construct the interior solution, we specify s^- and calculate the corresponding V from $dT(+\infty)/d\eta = 0$, after which it remains to integrate (3.2) and (3.6) and then to calculate $\Lambda(\eta)$ and $s(\eta)$ from the final relations of (3.5). One establishes the general form for $T(\eta)$ and $c(\eta)$ as follows. The right side in (3.6) is zero for $T = T^{\pm}$ or $\eta = \pm\infty$, and by virtue of (3.7) it is negative for $T^+ < T < T^-$, so $T(\eta)$ is a monotonically decreasing function tending asymptotically to $T^{\pm}$ for $\eta \to \pm\infty$. The Ω on the right in (3.2) is negative for $T < T_* = T^-$ in accordance with (2.3) and becomes zero for $T = T_*$ and $c = 0$, and in the latter case as c^n $(0 < n < 1)$, so for $c \to 0$ we have $dc/d\eta \sim c^n$ or $c^{n+1} \sim \eta + \text{const}$, i.e., $c(\eta)$ should become zero for the finite value $\eta = \eta^*$. Figure 3, curves 1 and 2, shows typical $T(\eta)$ and $c(\eta)$. For $\eta^* < \eta < \infty$, the right side in (3.6) is independent of c and is integrated in quadratures; then $\Lambda(\eta) \equiv \Lambda^+ = \text{const}$. For $-\infty < \eta < \eta^*$, the volume flow rate decreases from Λ^- to Λ^+ as η increases.

The interior-solution existence conditions amount to the continuity ones for $s(\eta)$ for $-\infty < \eta < \infty$. Let $s^* = s(\eta^*)$ and $T^* = T(\eta^*)$. We substitute $T = T^*$, $c = 0$, $K = 1$, $\Lambda = \Lambda^+$ into the first equation in (3.5) to get that the saturation s^* in the (s, G) plane, where

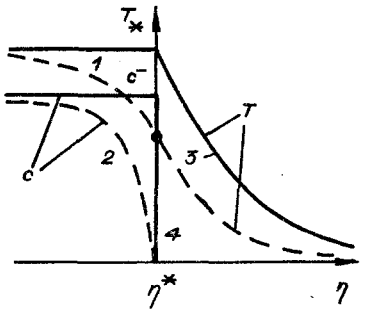

Fig. 3

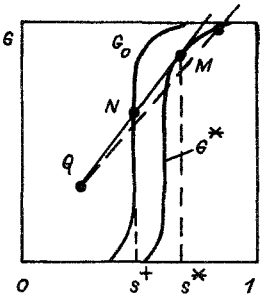

Fig. 4

G = ΛF, corresponds to the upper point of intersection M between the curve $G^*(s) = \Lambda^+ F(s, T^*, 0)$ and the straight line having slope V and passing through the point Q = (K^-s^-, K^-F^-) (Fig. 4). Then the s(η) in the hot water and oil zone ($\eta^* < \eta < \infty$) correspond to the points of intersection between MN and the same straight line between the lines $G_0(s) = \Lambda^+ F(s, 0, 0)$ and G*(s). The line $G_0(s)$ is derived from curve 1 in Fig. 1 by altering the vertical scale by the factor Λ^+. It is clear that MN should not intersect G*(s), since otherwise s as a function of T has a discontinuity at T = T*. The only possibility allowing s(T) to be continuous is that MN is tangential to G*(s) at M. As T* is dependent on s^-, the construction of the exterior and interior solutions is not decoupled at the principal term. Then the additional conditions are

$$V = \Lambda^+ F_s'(s^*, T^*, 0) = \frac{\Lambda^+ F(s^*, T^*, 0) - \Lambda^- K^- F^-}{s^* - K^- s^-}. \tag{4.1}$$

This result is analogous to that established previously [3] in the displacement of oil by an active solution with a nonmonotone dependence of the flow distribution on the component concentration. In the present case, the flow distribution is not monotonically dependent on the aqueous-phase specific heat content (Fig. 1), i.e., the best displacement conditions occur when hot water acts on the stratum, with the displacement completeness falling when steam is used because of reduced viscosity in the displacing phase, and also when cold-water displacement is used because of the increased oil viscosity. However, the spread in the thermal front due to thermal conduction and disequilibrium phase transition means that steam injected into the stratum always gives rise to a region where oil and hot water infiltrate in the displacement zone. Consequently, the performance is higher than is indicated by the displacement power of steam from curve 3 in Fig. 1. The above condensation-front step construction method incorporates this, although there is no hot water and oil infiltration region in the displacement zone when one constructs the solution in the large-scale approximation.

We now estimate ν/ε. From (2.4) we have $\nu/\varepsilon = (U^0)^2 \rho_1 (c_1 - c_2)/\lambda p \omega$. From [5], the ω introduced in (1.6) is about $6.3 \cdot 10^{-6}$ kg/(m³·Pa·sec). Then the maximum Ω = ωp for p = 10 MPa is estimated as 63 kg/m³·sec. We substitute λ = 2 kcal/m·h·°C, U^0 = 1 m/day, $\rho_1 = 10^3$ kg/m³, and $c_1 - c_2$ = 0.6 cal/cm³ into the expression for ν/ε to get ν/ε ≈ 0.0023, so thermal conduction is decisive by comparison with nonequilibrium effects as regards displacement.

The steam condenses instantaneously for ν/ε = 0, so the T(η) and c(η) distributions in the transition zone take the form shown by curves 3 and 4 in Fig. 3, which follows directly from (3.2) and (3.6) if one passes to the limit ν/ε → 0. Then the c(η) and s(η) distributions are discontinuous, with the discontinuities corresponding to the interior steam condensation front to give hot water at T = T_*. The T* appearing in (4.1) is not known in advance; it coincides with the transition temperature T_*, so one can construct the exterior solution without first defining the interior one. For $\nu/\varepsilon \geqslant 0$, the two characteristics in the first family diverge from the step line, so the step does not satisfy the evolutionary condition [12]. If steam completes the oil displacement (i.e., if the initial water content in the stratum s_0 is high), one gets the situation where s^+ should be larger than s*; then any solution to (3.1)-(3.3) for ν/ε > 0 is always continuous, and instead of (4.1) one puts $s^+ = s_0$ to close the step conditions.

5. Exterior Solution in the Absence of Heat Loss. If there is no heat exchange between the stratum and the surrounding rocks (a' = 0), there is a self-similar solution to (2.2)-(2.5) in the large-scale approximation (ε = ν = 0):

$$s = s(\xi), T = T(\xi), c = c(\xi), \Lambda = \Lambda(\xi), \xi = X/\tau. \tag{5.1}$$

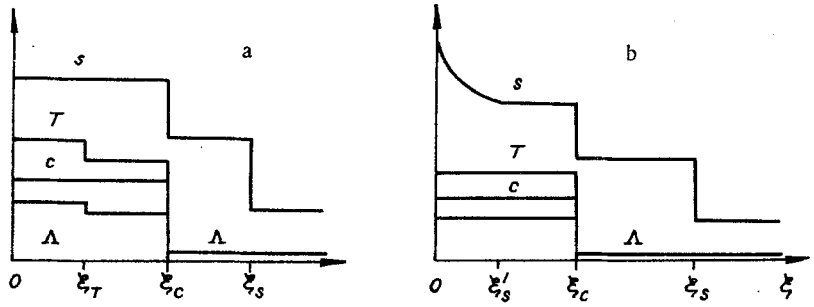

Fig. 5

Figure 5a shows a typical solution for superheated steam injection ($c^0 = 1$, $T_* < 1$); the $T(\xi)$, $c(\xi)$, and $\Lambda(\xi)$ curves are shown on different scales for greater clarity. There are three characteristic fronts in the displacement zone: steam cooling to the transition point — $\xi = \xi_T$, steam condensing — $\xi = \xi_c$, and cold-water displacement — $\xi = \xi_s$ ($\xi_T < \xi_c < \xi_s$). Also, s is constant in the infiltration zone for the superheated steam ($0 < \xi < \xi_T$) and the saturated steam ($\xi_T < \xi < \xi_c$), i.e., the oil is immobile behind the condensation front, which is a consequence of steam's low displacing power in a heated stratum and means that it is unsuitable to pump superheated steam into it. In fact, the displacement conditions are not thereby improved, while the volume heat content of the injected steam is reduced. When saturated steam is injected, the solution is similar, but there are no steps in T and Λ in the $0 < \xi < \xi_c$ zone. In a mixture of hot water and steam ($0 < c^0 < 1$), the displacement zone acquires a region of continuous saturation change (mobile oil region) $0 \leqslant \xi \leqslant \xi_s'$ (Fig. 5b). As the water concentration increases ($1 - c^0$), this region expands ($\xi_s' \to \xi_c$), and for $c^0 \to 0$, the solution goes over to the standard one for hot water displacing the oil [1, 2].

Only a qualitative displacement-zone structure description is given here. The solution is constructed in both cases (Fig. 5a and b) by configuring the step corresponding to the condensation front and satisfying (4.1) along with the conservation laws. The solution is completed in the usual way [2] when the condensation front parameters have been determined.

The step in the steam concentration c corresponding to the condensation front is always complete ($c^+ = 0$), and other steps in c at $T = T_*$ are impossible. This result applies also in the initial three-phase formulation. In particular, the oil displacement by steam zone in the absence of heat loss for $c^0 = 1$ does not contain regions of three-phase oil—water—steam flow. This is a further justification for using a pseudo-two-phase model. However, the solution is dependent on the internal condensation-front structure, so it does not follow that the solutions in the two models coincide.

In [4], there is a discussion of steam displacing oil with stratal heat transfer to the surrounding rock. It has been shown that the solution can be constructed everywhere apart from the stratum-heating zone, in explicit form. In the heating zone, the solution can be found numerically by the characteristic method. The proposed method has advantages over traditional ones in the preliminary front introduction, which eliminates the numerical-integration complexity for equations having discontinuous solutions.

I am indebted to K. M. Fedorov for initiating this study.

LITERATURE CITED

1. G. S. Braginskaya and V. M. Entov, "Nonisothermal oil displacement by an active solution," Izv. AN SSSR, Mekh. Zhidk. Gaza, No. 6 (1980).
2. V. M. Entov, Physicochemical Hydrodynamics in Porous Media: Models for Methods of Increasing Oil Recovery [in Russian], Preprint No. 161, IPM AN SSSR, Moscow (1980).
3. V. M. Entov and Z. A. Kerimov, "Oil displacement by an active solution that nonmonotonically influences the flow distribution," Izv. AN SSSR, Mekh. Zhidk. Gaza, No. 1 (1986).
4. A. F. Zazovskii and K. M. Fedorov, Oil Displacement by Steam [in Russian], Preprint No. 267, IPM AN SSSR, Moscow (1986).
5. O. A. Hougen and K. M. Watson, Chemical Process Principles, Vol. 3, Wiley, New York (1949).
6. C. Chu and A. E. Trimble, "Numerical simulation of steam displacement: field performance applications," J. Petrol. Technol., 27, No. 6 (1975).
7. B. L. Rozhdestvenskii and N. N. Yanenko, Quasilinear Equation Systems and Applications to Gas Dynamics [in Russian], Nauka, Moscow (1978).

8. G. I. Barenblatt, V. M. Entov, and V. M. Ryzhik, The Motion of Liquids and Gases in Natural Strata [in Russian], Nedra, Moscow (1984).
9. H. L. Beckers and G. J. Harmsen, "The effect of water injection on sustained combustion in a porous medium," Soc. Petrol. Eng. J., 10, No. 2 (1970).
10. O. M. Alishaeva, V. M. Entov, and A. F. Zazovskii, "The structure in conjugate saturation and concentration steps in oil displacement by active solutions," Zh. Prikl. Mekh. Tekh. Fiz., No. 5 (1982).
11. P. G. Bedrikovetskii and M. V. Lur'e, "Discontinuity stability and permissibility in equation systems for two-phase infiltration," Prikl. Mat. Mekh., 47, No. 4 (1983).
12. I. M. Gel'fand, "Some problems in quasilinear-equation theory," Usp. Mat. Nauk, 14, No. 2 (1959).

INCREASE IN WATER-HAMMER PRESSURE IN A PIPE IN THE PRESENCE OF A LOCALIZED VOLUME OF GAS

S. P. Aktershev and A. V. Fedorov

UDC 532.595.2+532.595.7

In different areas of use of piping systems, situations are often encountered whereby localized volumes of gas co-exist with the liquid in the pipe. The presence of the gas cavities may have a significant effect on the character of various transients in the pipeline [1-8]. Gas cavities may compensate for pressure fluctuations [2] or, conversely, may increase the maximum pressure in the pipe [3, 4]. The exact role played by the cavities depends on the parameters of the system and the method of organization of the nonsteady flow. As is known [1], the air chamber installed in the delivery line immediately after a pump reduces the pressure jump which occurs when the pump is started. On the other hand, when a capped pipe is filled with liquid, the presence of gas may lead to a water hammer of considerable magnitude [3]. The presence of air at the end of a delivery line with a closed valve may also result in large pressure fluctuations when the pump is quickly turned on [4].

The pressure-testing of a pipeline filled with a viscous liquid and provided with an air chamber (Fig. 1) was studied experimentally in [5] for large values of friction at the point of attachment of the chamber to the line. Valve A, connecting the line, under the pressure $\tilde{p}_0$, with a tank under constant pressure $\tilde{p}_1 > \tilde{p}_0$, was quickly opened at the initial moment of time. The air chamber was designed to damp the attendant pressure oscillations. The experimental data was compared with the results of numerical calculations. It was found that the maximum pressures were 1.5-1.8 times higher within a certain range of volumes of air in the chamber than in the absence of air. The results of the numerical calculations were used to determine the maximum permissible diameter of chamber throat that would ensure damping of pressure oscillations by the chamber for a specified volume of air.

Here we also examine the problem of the pressure-testing of a pipeline with a gas cavity. However, we will use small values of friction and assume that friction is concentrated in the initial section of the pipe (valve resistance). The effect of the volume of the gas cavity on the maximum pressures in the pipeline is studied both by a numerical method and within the framework of a simplified mathematical model proposed below.

Formulation of the Problem. The flow of liquid in the pipe is described by hydraulic equations [1] which appear as follows in the dimensionless variables $p = \tilde{p}/\tilde{p}_1$, $u = \tilde{\rho}_0\tilde{c}\tilde{u}/\tilde{p}_1$, $x = \tilde{x}/\tilde{L}$, $t = \tilde{c}\tilde{t}/\tilde{L}$

$$\frac{\partial p}{\partial t} + \frac{\partial u}{\partial x} = 0, \quad \frac{\partial u}{\partial t} + \frac{\partial p}{\partial x} + \alpha u|u| = 0, \quad \alpha = \lambda\tilde{L}\tilde{p}_1/(2\tilde{D}\tilde{\rho}_0\tilde{c}^2). \tag{1}$$

Here, $\tilde{p}$, $\tilde{u}$, $\tilde{\rho}_0$, $\tilde{x}$, $\tilde{t}$ are the dimensionless pressure, velocity, and density of the liquid, the longitudinal coordinate, and time; $\tilde{D}$, $\tilde{L}$, $\tilde{c}$ are the diameter and length of the pipe and the rate of propagation of perturbations in the pipe when it is filled with liquid; λ is the coefficient of friction against the wall. We assume that λ is constant, which is valid for Reynolds numbers $\mathrm{Re} \geqslant 10^5$ [9].

Novosibirsk. Translated from Zhurnal Prikladnoi Mekhaniki i Tekhnicheskoi Fiziki, No. 6, pp. 107-111, November-December, 1987. Original article submitted June 16, 1986.

0021-8944/87/2806-0899$12.50